Published in final edited form as:
J Am Chem Soc. 2011 April 27; 133(16): 6138–6141. doi:10.1021/ja200313q.

Chemical Patterning of Ultrathin Polymer Films by Direct-Write Multiphoton Lithography

Hojeong Jeon[a,**], **Ray Schmidt**[b,**], **Jeremy E. Barton**[b], **David J. Hwang**[a], **Lara J. Gamble**[c], **David G. Castner**[c], **Costas P. Grigoropoulos**[a,*], and **Kevin E. Healy**[b,d,*]

[a]Laser Thermal Laboratory, Department of Mechanical Engineering, University of California, Berkeley, CA 94720-1740, USA

[b]Department of Bioengineering, University of California, Berkeley, CA, 94720-1760, USA

[c]Department of Bioengineering, University of Washington, Seattle, WA, 98185

[d]Department of Materials Science and Engineering, University of California, Berkeley, CA 94720-1760, USA

Abstract

We applied 2-photon laser ablation to write sub-diffraction nanoscale chemical patterns into ultrathin polymer films under ambient conditions. Poly(ethylene glycol) methacrylate brush layers were prepared on quartz substrates via surface initiated atom transfer radical polymerization (SI-ATRP) and ablated to expose the underlying substrate using the non-linear 2-photon absorbance of a frequency doubled Ti:Sapphire femtosecond laser. Single-shot ablation thresholds of polymer films were ~ 1.5 times smaller than that of a quartz substrate, which allowed patterning of nanoscale features without damage to the underlying substrate. At a $1/e^2$ laser spot diameter of 0.86 μm the features of exposed substrate approached ~ 80 nm, well below the diffraction limit for 400 nm light. Ablated features were chemically distinct and amenable to chemical modification.

Patterned surface chemistry has been a driver in biological, sensor, optoelectronic, and electronic research for years. During this time parallel patterning techniques such as photolithography, microcontact printing, and imprint lithography have received much attention due to the rapid and relative ease of replicating a pattern.[1–3] Unfortunately, such techniques require master patterns, which are most often generated by expensive direct write laser patterning mask writers designed for the microelectronics industry.[4] Less elaborate and more readily accessible direct write approaches such as Electron Beam Lithography (EBL), Atomic Force Microscopy based Dip Pen Nanolithography (DPN), or Near-Field Scanning Optical Microscopy (NSOM) techniques allow the generation of arbitrary nanoscale patterns, an important feature for most experimental programs focused on nanoscale patterning, but fabrication times are limited by the processing environment and the dose time necessary to generate each feature.[4–6] While such techniques are sufficient for small experimental programs, the costs involved in generating the hundreds of large area samples with differing geometries needed for ambitious biological and sensor programs is often prohibitive.[7] For this class of applications there is a demonstrated need for a rapid direct write chemical patterning technology with low marginal cost. One potential method to

*Corresponding Authors: cgrigoro@me.berkeley.edu, kehealy@berkeley.edu.
**Equal Contribution

Supporting Information Available: Procedures for the synthesis of PEGMA films, laser ablation parameters, experimental analysis. This material is available free of charge on the internet at http://pubs.acs.org

achieve this speed is to extend conventional laser microfabrication technology, by exploiting multiphoton ablation, to reduce feature sizes below the optical diffraction limit.

Multiphoton lithography provides high-resolution material processing requiring neither photomasks nor chemical developers.[8,9] Intense femtosecond laser pulses can induce damage in transparent dielectrics by nonlinear absorption processes such as multiphoton initiated avalanche ionization.[10] In contrast to material modification by nanosecond or longer laser pulses, there is limited heat exchange during femtosecond laser pulse irradiation, which results in minimizing thermal stress and collateral damage. Therefore, the femtosecond laser induced ablation process is stable and reproducible.[11,12] In addition, due to the nonlinear optical characteristics and Gaussian beam profile of the femtosecond laser, structures smaller than the processing beam spot size can be fabricated by precisely adjusting the pulse energy close to the ablation threshold.[13,14] Since the laser interaction with dielectric materials is strongly nonlinear, a femtosecond laser focused via far-field optics can achieve ablative features with subwavelength resolution on inorganic (i.e. quartz) and polymer substrates (Fig. 1a).[8,13,15] To miniaturize feature sizes in polymeric materials, ultrathin films provide small interaction volumes and promote the formation of nanoscale features.

To produce ultrathin films with the tightly controlled thickness and low surface roughness critical in both the formation and characterization of nanoscale features, surface initiated atom transfer radical polymerization (SI-ATRP) was used.[16] As a living radical polymerization scheme, SI-ATRP films grow linearly, yield smooth homogenous films, and leave the terminal unit of the synthesized polymer as an active ATRP initiator, stable even after months on the shelf.[17] In this work 10–80 nm thick polyethylene-glycol monomethacrylate (pEG) polymer brush layers, chosen for robust non-fouling behavior, were generated by SI-ATRP on quartz, then ablated by single femtosecond laser pulses to expose the underlying substrate. By processing close to the ablation threshold under multiphoton absorption conditions, patterns with sub-diffraction feature diameters were rapidly obtained under ambient conditions in a direct-write method.

To examine the film growth kinetics, the SI-ATRP polymerization was monitored *in situ* using a quartz crystal microbalance with dissipation monitoring (QCM-D). SI-ATRP generates a uniform thin film which grows at ~1 nm per hour, and yields an average surface roughness of 0.9 nm RMS. Addition of Cu(II) ATRP deactivator complex prevented chain termination and ensured a living polymerization.[18] The reaction proceeded linearly with time, then deviated from linearity after approximately 400 minutes, as shown in Figure 1b. The deviation was attributed to deactivation of the catalyst system by slow leakage of oxygen into the QCM-D chamber. Reflectometry measurements of the film thickness revealed a linear increase in film thickness of 1 nm/hour for more than 40 hours (Fig. S1). This linear growth rate provided uniform and controllable polymer films critical for laser ablation experiments. The surface chemistry of the polymer thin film was verified by x-ray photoelectron spectroscopy (XPS). Following growth of a pEG brush layer, a large peak resulting from the C-O species was prevalent, verifying the reaction produced a PEG film (Fig. S2).

Nanoscale features in the pEG films were generated by user-designed rastering of a sample through the beam path while applying pulses synchronized with the sample translation. Depending upon the desired pattern arrangement, either single laser pulses were fired by the laser at specified times, or a fixed number of pulses were allowed via a mechanical shutter from a train of pulses (maximum frequency is 1kHz) while the translation stage was rastered (see, details in SI). To determine the ablation thresholds of both the polymer and the underlying quartz substrate for our particular system, samples were ablated at progressively

decreasing pulse energies. The ablation threshold of the pEG brush layer was lower than that of the underlying quartz substrate, creating an ideal processing window between 4~4.5 nJ. For example, for a 100x objective in which only the 14-nm polymer film was ablated, features of exposed substrate approached ~80 nm (Fig. 2a,b). AFM images of the ablated surfaces, as well as high-resolution images of single features, as shown in Figures 1c and 2a, demonstrate the regularity of features at or above 4.5nJ with a 100x objective.

The processing energy was dependent on the optics of the system (one relevant metric is the numerical aperture), yielding a multi-photon absorption dependent film ablation threshold energy density of ~0.8 J/cm^2 with a 100x objective. At pulse energies above 5 nJ, damage to both the pEG layer and the underlying quartz substrate was observed (Fig. 2b). Using Eq. 1 (SI) and the calculated radii of the laser beam (w_0) (0.43, 0.66, and 2.05μm for 100x, 50x, and 10x objectives, respectively), the ablation thresholds were calculated to be ~ 0.6 to 1 J/cm^2 for the pEG film and ~ 1.2 to 1.5 J/cm^2 for quartz substrate, respectively (Fig S2). At fluences between the ablation threshold of the film and quartz, only the polymer film was removed to expose the underlying quartz substrate.

The minimum feature sizes depended on the film thickness (Fig. 2c): thinner films yielded smaller features, particularly with high NA objectives (Fig. S2). This effect was used to generate a wide range of feature sizes by tuning the laser energy and the film thickness. The minimum crater bottom diameters for a 10-nm thick film using 10x, 20x, and 50x objectives were ~730 nm, ~370 nm, and ~160 nm, respectively, and ~80 nm by a 100x objective with a 14-nm film. This patterning proceeded simply and rapidly at 100–1000 Hz, under ambient conditions. While the minimum feature sizes were determined for a single laser shot at a specific wavelength triggering the two-photon absorption process, further improvement in spatial resolution is expected by more rigorous testing with other laser parameters such as number of shots, wavelength, and temporal/spatial beam profiles. Optimization of polymer film characteristics for higher quality of ablation is another route (e.g. one can manipulate the optical, chemical, thermal, and mechanical properties of the film).[19,20] Nevertheless, the wide range of parameters examined in this study support multi-scale feature selectivity with convenient processing windows, avoiding either unwanted substrate damage or exploiting controlled damage for three-dimensional effects.

To verify the localized chemical contrast following ablation of the polymer thin film, the protein Neutravidin was physisorbed to the crater bottom and then tagged with a fluorescently labeled biotin, resulting in patterns shown in Fig. 3. Localized regions of fluorescence were observable down to 300 nm diameter features (Fig. 3b). Comparing the tapping mode AFM of the dried samples before and after protein deposition reveals a 3–4 nm change in the average crater depth, indicating selective protein adsorption (Fig. 3c,d). AFM indicated little deposition of protein onto the polymer walls of the crater suggesting minimal damage to the polymer structure by sub-threshold exposure to the fs laser beam and the ejected plume generated by the ablation process.[21]

Finally, we applied this chemical pattering technique to control the adhesion and migration of 3T3-fibroblasts by defining the surface density of ligands for cell surface adhesion receptors (i.e., integrins). We adsorbed Neutravidin protein to the exposed quartz regions defined by the laser ablation pattern, and to the nanopatterned protein we then immobilized a biotin tagged peptide encoding the bone sialoprotein RGD integrin binding domain (bsp-RGD(15): biotin-GGNGEP**RGD**TYRAY).[22] By defining a pattern with a constant 500 nm ablation diameter and varying the pitch between features, we were able to vary the peptide surface density from 2.5 pmol/cm^2 to 0.02 pmol/cm^2. Time-lapse microscopy revealed that seeded cells settled onto the high ligand density region of the gradient, rapidly attached to the surface and spread, while cells that settled onto the low density regions of the gradient

had difficulty adhering, did not spread significantly, and migrated to the high ligand density regions of the gradient (Figure 4, S5, and M1). Based on the position of the cells after 20h, which includes both cell adhesion to and migration on the gradient nanopattern, these 3T3-Fibroblast cells preferred a minimal peptide surface density of at least 0.15 pmol/cm^2.

Future developments of this technique will focus on increasing the patterning rate, decreasing the feature size through chemical post-processing, expanding the pool of polymer materials, and applying the chemistry of the polymer ablation to generate chemical contrast without exposing the underlying quartz. One project of particular interest is to expand the use these patterned substrates to control cell adhesion and explore mechanisms of mechanobiology.

We have determined the chemical, physical, and optical parameters necessary to pattern methacrylate based polymer thin films at sub-diffraction resolutions, and we have applied this system to generate biologically active nanoscale regions of chemical contrast. SI-ATRP provides precise control over the film thickness and uniformity, particularly important parameters for patterning nanoscale features. This first-generation direct write technique is a thousand times faster than comparable versatile ambient air techniques like DPN and NSOM and speed, resolution, and material capabilities can only improve in future implementations using, for example, higher pulse repetition frequency laser sources. Ultimately the high speed sub-diffraction patterning capabilities of fs laser ablation can be combined with the post-processing potential of SI-ATRP synthesis to produce myriad versatile chemical patterning techniques.

Supplementary Material

Refer to Web version on PubMed Central for supplementary material.

Acknowledgments

National Institute of Health (N.I.H.) grants GM085754 and HL096525 (K.E.H. & C.P.G.). The XPS experiments were performed at the National ESCA and Surface Analysis Center for Biomedical Problems, which is supported by NIH grant EB-002027 (D. G. C, L. J. G.). We thank Professor Ting Xu of the Department of Materials Science at the University of California, Berkeley, for use of the Fibermetrics thin-film analyzer.

References

1. Lom B, Healy KE, Hockberger PE. Journal of Neuroscience Methods. 1993; 50:385. [PubMed: 8152246]
2. Kumar A, Whitesides GM. Applied Physics Letters. 1993; 63:2002.
3. Chou SY, Krauss PR, Renstrom PJ. Science. 1996; 272:85.
4. Menon R, Patel A, Gil D, Smith HI. Materials Today. 2005; 8:26.
5. Piner RD, Zhu J, Xu F, Hong S, Mirkin CA. Science. 1999; 283:661. [PubMed: 9924019]
6. Chimmalgi A, Hwang DJ, Grigoropoulos CP. Journal of Physics: Conference Series. 2007; 59:285.
7. Schmidt RC, Healy KE. Journal of Biomedical Materials Research Part A. 2009; 90A:1252. [PubMed: 19585563]
8. Higgins DA, Everett TA, Xie AF, Forman SM, Ito T. Applied Physics Letters. 2006; 88
9. Ibrahim S, Higgins DA, Ito T. Langmuir. 2007; 23:12406. [PubMed: 17960946]
10. Grigoropoulos, CP. Transport in Laser Microfabrication: Fundamentals and Applications. New York: Cambridge University Press; 2009.
11. Chichkov BN, Momma C, Nolte S, vonAlvensleben F, Tunnermann A. Appl. Phys. A-Mater. Sci. Process. 1996; 63:109.
12. Stuart BC, Feit MD, Rubenchik AM, Shore BW, Perry MD. Physical Review Letters. 1995; 74:2248. [PubMed: 10057880]

13. Korte F, Serbin J, Koch J, Egbert A, Fallnich C, Ostendorf A, Chichkov BN. Applied Physics a-Materials Science & Processing. 2003; 77:229.
14. Hwang DJ, Grigoropoulos CP, Choi TY. Journal Of Applied Physics. 2006; 99
15. Hartmann N, Franzka S, Koch J, Ostendorf A, Chichkov BN. Applied Physics Letters. 2008; 92:3.
16. Patten TE, Matyjaszewski K. Advanced Materials. 1998; 10:901.
17. Tugulu S, Barbey R, Harms M, Fricke M, Volkmer D, Rossi A, Klok H-A. Macromolecules. 2006; 40:168.
18. Pyun J, Kowalewski T, Matyjaszewski K. Macromolecular Rapid Communications. 2003; 24:1043.
19. Lippert T, Hauer M, Phipps CR, Wokaun A. Applied Physics A: Materials Science & Processing. 2003; 77:259.
20. Lippert T, Dickinson JT. Chemical Reviews. 2003; 103:453. [PubMed: 12580639]
21. Choi TY, Grigoropoulos CP. Journal Of Applied Physics. 2002; 92:4918.
22. Rezania A, Thomas CH, Branger AB, Waters CM, Healy KE. Journal of Biomedical Materials Research. 1997; 37:9. [PubMed: 9335344]

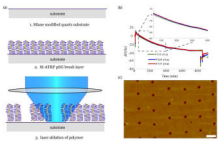

Figure 1.

(a) Schematic of laser ablation. Polymer is grown from surface bound ATRP initiator and ablated by a 100 fs 400 nm laser pulse. (b) QCM-D measurement of polymer thickness over time indicates linear growth of the living radical polymerization, ensuring the smooth uniform films necessary for consistent laser ablation. (c) AFM image of 250 nm dot pattern in 20 nm film demonstrates unform feature sizes (scale bar is 1 μm).

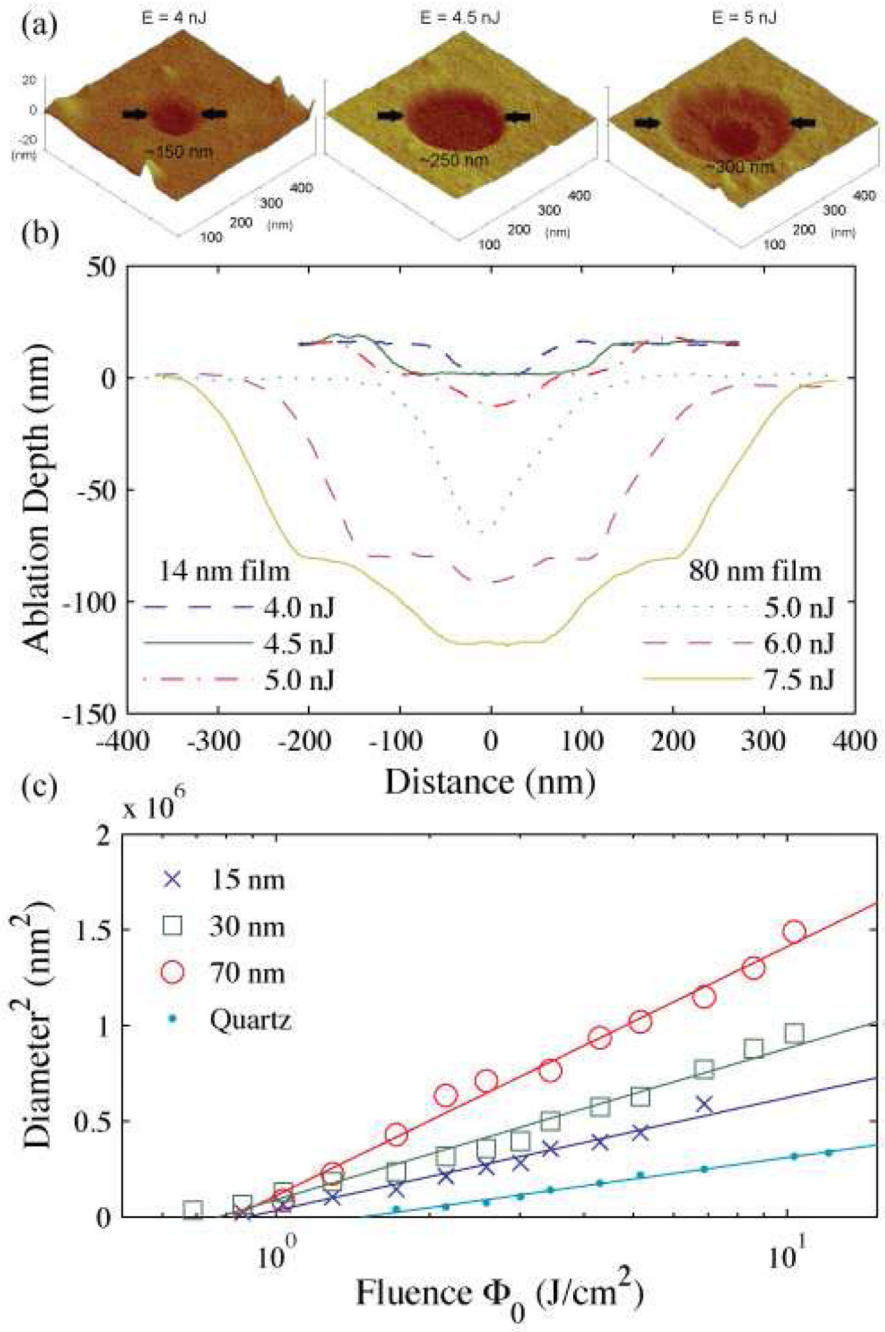

Figure 2.

(a) Representative AFM scans of polymer ablation craters in a 14 15 in paper? nm thick film at 4 nJ, 4.5 nJ, and 5 nJ. In the 5 nJ crater one can clearly see the ablated quartz in the middle of the feature. (b) Tracing the cross section of features ablated into 14 and 80 nm thick films shows the effect of increasing energy and film thickness very clearly. The 14 nm thick film is offset up by 15 nm. For a given objective (100x in this case) and beam profile, (c) shows that the thickness of the film increases the feature size at all energy densities

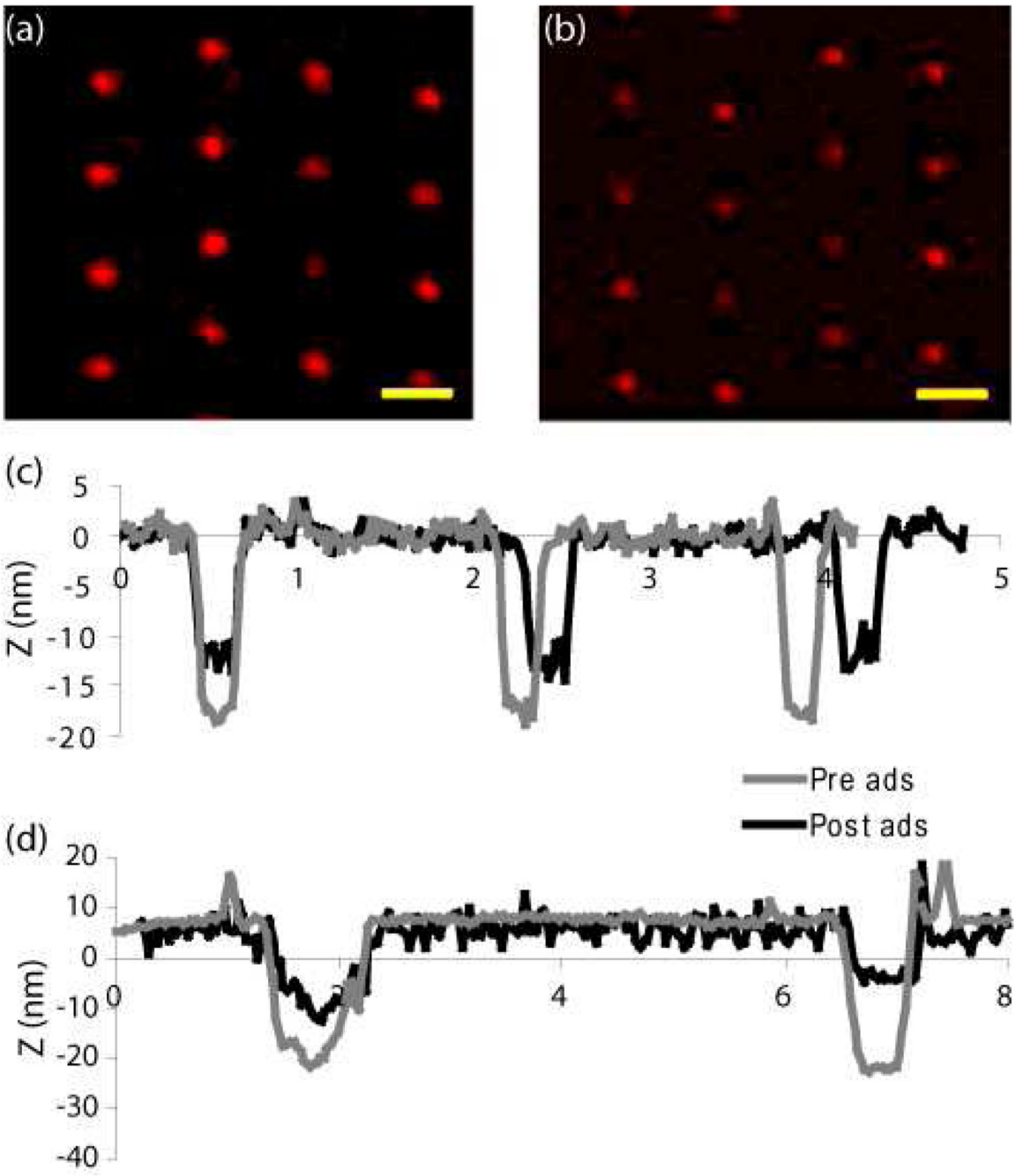

Figure 3.
Confocal fluorescence of selectively adsorbed Neutravidin bound to fluorescently labeled biotin in a) 500 nm and b) 300 nm diameter features. Scale bar = 1 μm c) AFM cross sections of features before and after c.) Neutravidin and d) Fibronectin protein adsorption.

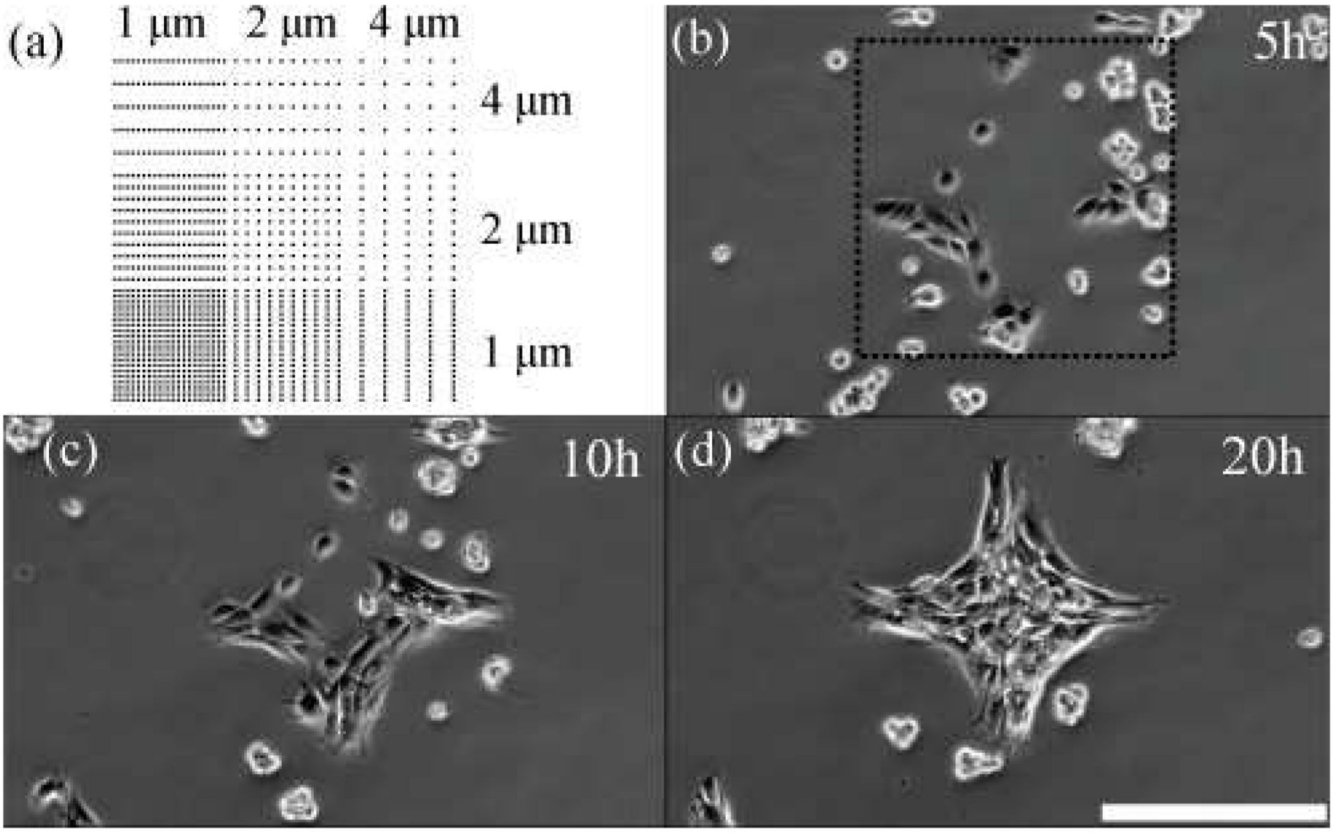

Figure 4.

(a) Schematic of the ablated pattern with 500 nm dots on a variable pitch. This diagram shows the inner part of one quadrant of the total pattern, which is mirrored into the other three quadrants around the lower left corner. A more detailed image (S4) is in SI. The pitch between features varied between 1 μm and 10 μm. (b) 5 hours after cells were seeded onto the pattern, they attached and spread on areas of higher density. The dashed box reveals the boundaries of the pattern. (c) and (d) are 10 and 20 hour time points, that demonstrate robust cell residence only on high density areas of the pattern with a surface peptide concentration of at least 0.15 pmol/cm^2. Movie (M1 in SI) indicates cells did attach to the low surface density regions, then migrated as either individual cells or cell aggregates to the higher density regions.